MR 영상 신호의 자화율 효과 분석

노용단[1], 홍인기[2], 조장희[2,3]

1) 대전대학교 전산학과 2) 한국과학기술원 정보통신공학과 3) 켈리포니아대학 방사선학과

Analysis of Susceptibility Effect in MR Image Signal

Y.M.Ro[1], I.K.Hong[2], Z.H.Cho[2,3]

1)) Dept. of Computer Science, Taejon University, 96-3 Yongwoon-dong Dong-gu, Taejon, Korea, 2) , Korea Advanced Institute of Science, P.O.Box 201, Cheongyangni, Seoul, Korea, 3) , Dept. of Radiological Sciences, University of California, Irvine, CA92717,

I. *INTRODUCTION*

Magnetic susceptibility differences between materials produce magnetic field variations at their interfaces. Since the susceptibility generated field inhomogeneity is highly localized and relatively strong compared with other field inhomogeneities spins in a voxel become incoherent, resulting in a significant signal intensity reduction, in paricular for large voxel. In NMR imaging, the effects lead to geometrical deformation and signal reduction (1). The latter, especially the signal reduction caused by spin dephasing within a voxel, is well known and has been a subject of several articles (1-4).

The signal loss phenomenon is especially noticeable in gradient echo imaging. A correction method for the signal reduction due to the susceptibility effect using tailored RF pulse was recently reported by the present authors (2). More recently, the signal loss phenomenon due to susceptibility was utilized for susceptibility contrast or T2* contrast in functional imaging and venography in conjunction with gradient echo technique (3) . Its further applications to functional imaging brought about new dimensions in NMR imaging (4). Since the venous blood contrast is easily seen in the conventional gradient echo imaging due to the fact that the venous blood contains deoxyhemoglobin which has paramagnetic properties.

In this paper, we propose a new spectral decomposition technique which is applicable to the analysis of the susceptibility affected signal. Since the signal intensity is changed by the susceptibility effect, spectral decomposition of the signal intensity will reflect the susceptibility effect. Therefore, the method can be used for generalized susceptibility effect analysis in MR imaging. A demonstrating is carried out using a 2.0 T whole body NMR system, and the result is utilized for venography. Computer simulations as well as experimental studies are carried out to validate the methods and demonstrate the applicability of the method in venography, and possibly in functional imaging (6).

II. THEORY

1. *The Spectral Decomposition of the susceptibility Affected Signal*

As previously discussed, the field variation produced by the susceptibility effect is usually quite large, so that even spins within a single voxel experience a large inhomogeneous field. On the other hand, the spins from the normal tissue experience a homogeneous field. In general, the image signal for a given pixel (x_i, y_j) in a 2-dimensional image is a complex function and can be written as

$$\rho(z; x_i, y_j) = m(x_i, y_j) \exp[i\phi(z; x_i, y_j)] \text{rect}\left(\frac{z}{z_0}\right) \qquad [1]$$

Note that Eq. [1] represents the intravoxel signal at a given pixel position (x_i, y_j) and is a function of z (slice selection direction) only.

Where $m(x_i, y_j)$ and $\phi(z; x_i, y_j)$ are the magnitude and phase distribution of spins in the selected voxel (x_i, y_j), respectively, and z_0 is the slice thickness. Eq. [2] shows the contribution to the signal intensity of the pixel at (x_i, y_j) from spins at position (x, y, z). The pixel intensity in the image, therefore, is given by summing $\rho(.)$ over the entire voxel.

In Eq. [2], the phase distribution, $\phi(z; x_i, y_j)$ is generated by the field inhomogeneity. Intravoxel signals of normal tissues, the phase term of Eq. [2] would be constant because the spin phases within the voxel will be coherent. If a voxel is located in an extremely inhomogeneous region, the phase term will not be constant even within a voxel. Furthermore, the strength of the phase term represents the extent of the susceptibility effect; the greater the susceptibility effect on the intravoxel signal, the bigger the phase variation. Therefore, the phase term of intravoxel signal, except the constant phase, is a complex value composed of many different degrees of susceptibility gradients or effects.

Let us now perform spectral decomposition of the above intravoxel signal. Fourier transform of Eq. [1] is performed in reference to the z-direction since the susceptibility affected signal is assumed to be variable only in the z-direction (2,3). Spectral decomposition is then equivalent to the one dimensional NMR imaging or Fourier transform for a given point (x_i, y_j) with ω_z was a parameter, i.e.,

$$S(\omega_z; x_i, y_j) = F[\rho(z; x_i, y_j)]$$
$$= \int_{-\infty}^{\infty} m(x_i, y_j) \text{rect}\left(\frac{z}{z_0}\right) \exp[i\phi(z; x_i, y_j)] \exp[-i\omega_z z] dz \qquad [2]$$

where F[.] is the fourier transform operator and ω_z is the spectral domain representation of the susceptibility effect. For the detailed analysis, the following two cases are considered.

Case I. A simple linear phase induced by the susceptibility effect.

Let us first consider the case where the phase term $\phi(z; x_i, y_j)$

is linear. Since the field inhomogeneity due to the susceptibility is highly localized and abrupt, the susceptibility induced field gradient induced by the susceptibility effect within a thin slice can often be considered as a linear gradient (1,2,3). Consequently, the phase distribution due to the susceptibility can also be considered linear along the slice selection direction z, i.e.,

$$\phi\left(z; x_i, y_j\right) = \gamma\, T_E G_{SUS}\left(x_i, y_j\right) z = P_{SUS}\left(x_i, y_j\right) z \qquad [3]$$

where γ is the gyromagnetic ratio, T_E is the echo time, $G_{SUS}(x_i,y_j)$ is the field gradient generated by the susceptibility gradient, i.e., $P_{SUS}(x_i,y_j) = \gamma T_E G_{SUS}(x_i,y_j)$.

If the phase term in Eq.[2] is replaced by a linear phase given in Eq. [3], Eq. [2] can be written as

$$S\left(\omega_z; x_i, y_j\right) = z_0 m\left(x_i, y_j\right) \operatorname{sinc}\left[\frac{\left\{\omega_z - P_{SUS}\left(x_i, y_j\right)\right\} z_0}{2\pi}\right] \qquad [4]$$

The term $\operatorname{sinc}[\{\omega_z - P_{SUS}(x_i,y_j)\} z_0/2\pi]$ in Eq. [4], therefore, means that the spectrum which appears as sinc function is now shifted by an amount $P_{SUS}(x_i,y_j)$ for the pixel at (x_i,y_j). This suggests that the susceptibility affected signal can be decomposed by P_{SUS} components in spectral domain. Equation [4], therefore, represents the spectrally resolved intravoxel signal affected by a single susceptibility gradient.

Case II. A composite phase representing the higher order nonlinear phase induced by the susceptibility Effect.

Since any complex nonlinear phase distributions can be decomposed by sum of linear phase distributions, the phase distribution given in Eq. [2] can be considered as a general phase distribution which can be a composite of many linear phase distributions. Therefore, in practice, the phase term $\phi(z;x_i,y_j)$ may not be linear for the z-direction, although the linear assumption mentioned in Case I is a reasonable assumption in many 2D imaging imaging situations. Let us consider the general case that is the nonlinear, in order to generalize the spectral decomposition for susceptibility affected signal analysis. For simplicity, let us define the term $\exp[i\phi(z;x_i,y_j)]$ as f(z) and let it represents a general phase function which can be written as a fourier series with fourier coefficients and phase factors within the slice thickness ($-z_0/2$ to $z_0/2$), i.e.,

$$f(z) = \exp\left[i\phi\left(z; x_i, y_j\right)\right] = \sum_{n=-\infty}^{\infty} f_n \exp\left[i\omega_n z\right] \qquad [5]$$

where ω_n is $2\pi n/z_0$, and n is integer, and f_n is a Fourier coefficient which is obtained by Fourier transform of f(z).

Equation [5] suggests that the phase term of the susceptibility affected signal f(z) can be represented as a sum of the linear phases ($\exp[i\omega_n z]$) in the z-direction. This is an important conclusion that can be used for the analysis of complex susceptibility dependent phase distribution, since it suggests the possibility of analyzing any complex susceptibility affected signals in the form of linear phases. Now, using Eq. [5], Eq. [2] can be rewritten as,

$$S\left(\omega_z; x_i, y_j\right) = m\left(x_i, y_j\right)\int_{-\infty}^{\infty} \operatorname{rect}\left(\frac{z}{z_0}\right)\sum_{-\infty}^{\infty} f_n \exp\left[i\omega_n z\right]\exp\left[-i\omega_z z\right] dz$$

$$= z_0 m\left(x_i, y_j\right)\sum_{-\infty}^{\infty} f_n \operatorname{sinc}\left[\frac{\left(\omega_z - \omega_n\right) z_0}{2\pi}\right] \qquad [6]$$

Note that both ω_z and ω_n in Eq. [6] represent the spectral frequency, but, the Fourier coefficients, ω_n represent the spectral frequency of discrete form. Although Eq. [6] indicates that $S(\omega_z;x_i,y_j)$ is represented as a series of sinc functions with varying coefficients, the series in the summation term will converge to a single term

which corresponds to $\omega_z = \omega_k$ and will have an amplitude $z_0 m(x_i,y_j) f_k$. As shown in Eq. [6], therefore, the intravoxel signal affected by the susceptibility can be decomposed into the spectral components, but one at each time, i.e., only at $\omega_z = \omega_k$. That is each of which represents a different intensity f_n and which in turn corresponds to a given susceptibility strength ω_n ($\propto G_{SUS}T_E$). Therefore, after n-steps of encoding, n susceptibility spectra or susceptibility Phase gradients can be obtained. These spectra or phase gradients, in turn provide unique information on susceptibility effect in imaging, that is the susceptibility component values of imaging voxel. Utilizing this method, images with varying degrees of susceptibility effect can also be obtained by summing the appropriate numbers of spectral components once the entire spectrum of the intravoxel signal is obtained. As an application of the method, susceptibility imaging utilizing this spectral decomposition technique is discussed in the following.

2. Computer simulation of the spectral decomposition in susceptibility imaging

In order to demonstrate the applicability of the spectral decomposition method in susceptibility imaging, computer simulations were performed with a phantom which has a spherical geometry as shown in Fig. 1. For the sake of simplicity, we have chosen a spherical geometry whose susceptibility induced field inhomogeneity is already known (5). In the simulations, an air sphere with radius R (=5cm) is assumed to be located at the center of the homogeneous water bath (see Fig. 1). By solving the magnetic scalar potential, the external field B_e in z-direction, which is superimposition with B_0, can be calculated by

$$B_e = B_0\left[1 - \frac{\mu_w - \mu_o}{2\mu_w + \mu_o}R^3 \frac{2z^2 - x^2 - y^2}{r^5}\right] \qquad [7]$$

where $r^2 = x^2 + y^2 + z^2$ and B_0 is the main magnetic field, and μ_w and μ_o are permeabilities of water and air, respectively..

For the imaging, a plane $(x,y;z=z_0)$ located at near the center of the sphere (1 cm above the z=0 plane) in the z-direction is selected as shown in Fig.1. The thickness of the slice and radius of the sphere were chosen to be 1 cm and 5 cm, respectively. The slice thickness is assumed to be a rectangular function. 32 spins are assumed in each voxel in the selected slice (in z-direction). From Eq. [6], it is noticed that the spins in a voxel far from the center of the sphere or the interface, e.g., in the case of $r^5 >> 2z^2-x^2-y^2$, field would be more or less a constant value, B_0. Fig. 2 shows the phase distributions of the spins in each voxel (32 spins) at several different x locations (see indicated positions $x_1 \sim x_6$ in Fig. 1) within the slice induced by the susceptibility effect. As shown in Fig.3, the spin phase distributions of some voxels (e.g. x_5, x_6) near the interface region are not only somewhat broader than ones far from the interface regions (e.g. x_1, x_2) due to the broader distribution of inhomogeneity or field gradients, but peak is shifted substantially as distances get close to the interface region. As explained earlier, shifts of peak values of the phase gradients, as the voxels approach to the interface (e.g. x_5, x_6) are much greater than the ones (voxels)at far from the interface. In spite of these variations in the phase distributions, most of the phase distributions within a voxel are relatively linear in z-direction due to the relatively thin slice (10 mm thickness).

Let us now perform the spectral decomposition with the susceptibility affected signals of the ones shown in Fig. 2. The results are shown in Fig. 3 for each different phase distribution. As expected, the intravoxel signals having small phase variation in the voxel are decomposed into a narrow spectral resolution at low ω_z

value, while the signals having large phase variation are distributed with somewhat broader spectral resolution at higher ω_z values. The results show that, in the spectral domain, the mean spectral or peak value ω_z represents the strengths of phase gradients or the extent of susceptibility effect in each voxel. That is, the higher the mean spectral value ω_z (e.g., $\omega_z = -7.5\ \pi$), the more severely the voxel is affected by the susceptibility effect. Finally, spectrally decomposed images corresponding to Fig.3 are obtained and shown in Fig. 4. As it is implied, the high spectral domain images (large ω_z values) represent high susceptibility effect or susceptibility gradient images , while the low (near $\omega_z = 0$) spectral domain images represent low susceptibility gradient images. The latter represents more like the normal tissues than the susceptibility affected regions such as the interface regions between the venous blood vessels and their surrounding tissues or mixtures of the two.

III. EXPERIMENTAL RESULTS AND DISCUSSIONS

Experiments were carried out using the 2.0 T whole-body NMR imaging system. To observe the possibility of susceptibility effect imaging by use of the proposed spectral decomposition method, imagings were performed with human volunteers. A sagittal view of a head section was selected in the vicinity of sagittal sinus to visualize the venous blood (deoxyhemoglobin). The pulse sequence used is shown in Fig.5. First, when m=0 or $\Delta T=0$ is used, it corresponds to the conventional gradient echo imaging. When $m \neq 0$, a series of high order susceptibility effect images will be obtained. In this experiment, repetition time and echo times were 70 msec and 25 msec, respectively with a slice thickness of 10mm. When RF pulse shifting was incorporated with $m\Delta T = -800, -600, -200, 200, 600,$ and 800 μsec, six spectrally resolved images were obtained. Since slice selection gradient (z-gradient) was 0.2 gauss/cm if each RF pulse shifting is 100 μsec, the maximum phase difference within the voxel (i.e., z=10mm thickness) for each step will be 0.535 radian.

Six spectrally decomposed images obtained are shown in Fig.6 with spectral components corresponding to $\omega_z = -4.28, -3.11, -1.07, 1.07, 3.11,$ and 4.28 radian/cm. As shown in Fig. 6, most of the veins or probably the surroundings of the veins, which would show strong susceptibility gradients, appear at the higher ends of the spectrum. Vicinities of venous blood appear in the high spectral component images such as the images at $\omega_z=-4.28$, and 4.28 radian/cm. On the other hand, the other normal brain tissues, which is believed to be not affected by the susceptibility, appear in the lower ends of the spectral components, e.g., $\omega_z= -1.07$, and 1.07 radian/cm. This means that the images at the higher spectral components are the ones affected most by the stronger susceptibility effects, i.e., the higher the spectral components, the stronger the susceptibility effect or gradients. Note also that at the high spectral regions, the signals of the normal tissues are mostly suppressed and only the signals from the regions which are affected by the susceptibility are enhanced.

In conclusion, a new susceptibility effect imaging technique using spectral decomposition has been proposed and experimentally studied. Results obtained by computer simulations and experiments show that the susceptibility affected images can be decomposed into discrete spectral component images, which are specifically related to the susceptibility effects in the voxels of the image. This method is, therefore, potentially useful for susceptibility imaging and analysis of susceptibility affected signals. It is also possible to apply this method in the areas of functional MR imaging where the basic

contrast mechanism is believed to be based on the susceptibility effect, such as the venous blood which contains deoxyhemoglobin. Since the method is capable of providing relatively quantitative information regrading the state of the susceptibility effect or local susceptibility gradient, it can be used for the collection of the precursory data from which an optimum parameter for susceptibility functional imaging can be derived (3,4).

IV. REFERENCES

1. H.W.Park, Y.M.Ro and Z.H.Cho, Phys.Med.Biol., 33, 339, 1988
2. Z.H.Cho and Y.M.Ro, Magn. Reson. Med. 23, 193, 1992
3. Z.H.Cho, Y.M.Ro and T.H.Lim, Magn, Reson. Med. 28,25,1992
4. Z.H.Cho,Y.M.Po,P.Ong et al, Twelveth SMRM,1406,1993.
5. K.M.Ludeke et al, Magn.Reson.Img.3,329,1985.
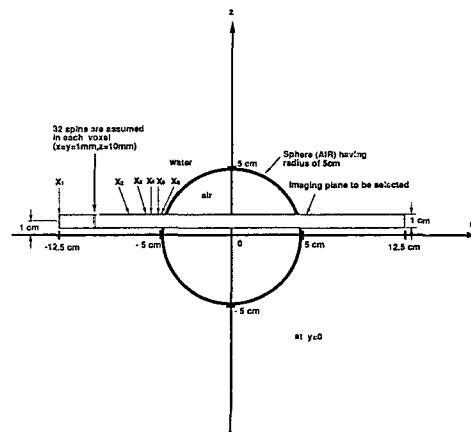6. S.Posse, Magn.Reson.Med.25,12.1992.

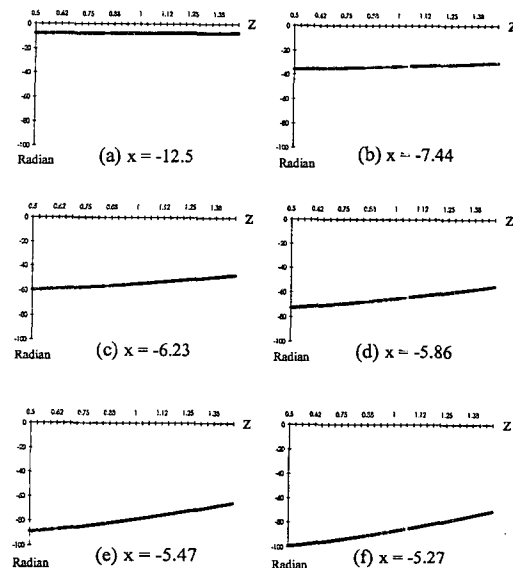Fig.1 A phantom used in the computer Simulations.

Fig.2 Phase distributions of the spins within a voxel at different x locations in the selected slice.

(a) $x_1 = -12.5$

(b) $x_1 = -7.44$

(c) $x_1 = -6.23$

(d) $x_1 = -5.56$
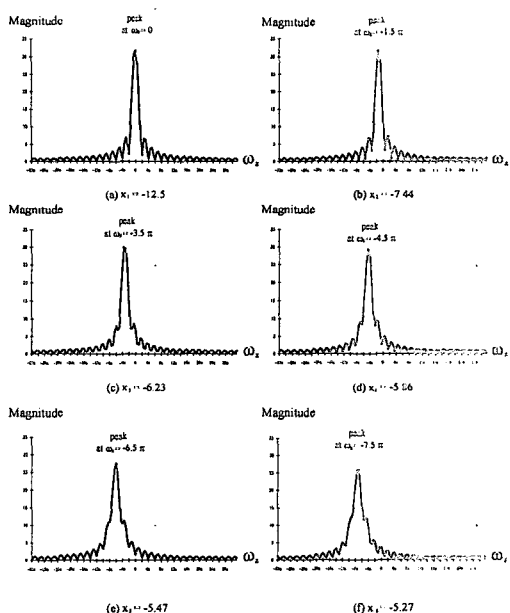
(e) $x_1 = -5.47$

(f) $x_1 = -5.27$

Fig.3 Decomposition spectra of the susceptibility affected signals in the selected slice (each spectrum corresponds to the phase distribution shown in Fig.2)
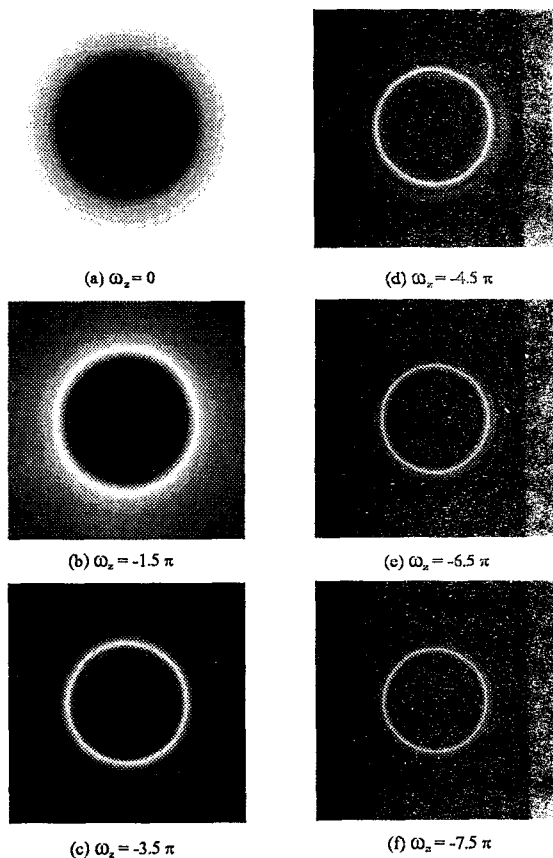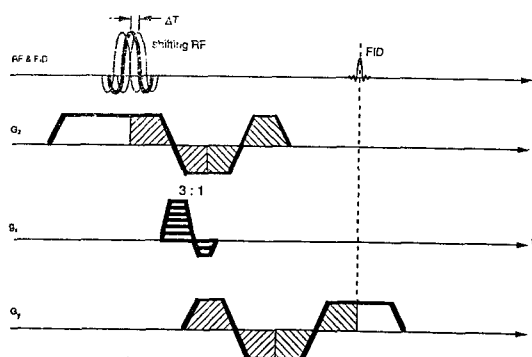

Fig.5 The actual pulse sequence applied in the experiments. In this sequence, we have employed RF time position shifting (mΔT) instead of varying g_z. This method requres m RF time position shifts if we desire to have m-spectrally decomposed images. Note that g_z is kept to a constant value G_z and only mΔT is varied.

(a) $\omega_z = 0$

(b) $\omega_z = -1.5\pi$

(c) $\omega_z = -3.5\pi$

(d) $\omega_z = -4.5\pi$

(e) $\omega_z = -6.5\pi$

(f) $\omega_z = -7.5\pi$

Fig.4 The Spectrally decomposed images of the selected slice

(a) $\omega_z = 1.07$ (Rad/cm)

(b) $\omega_z = -1.07$ (Rad/cm)

(c) $\omega_z = 3.11$ (Rad/cm)

(d) $\omega_z = -3.11$ (Rad/cm)

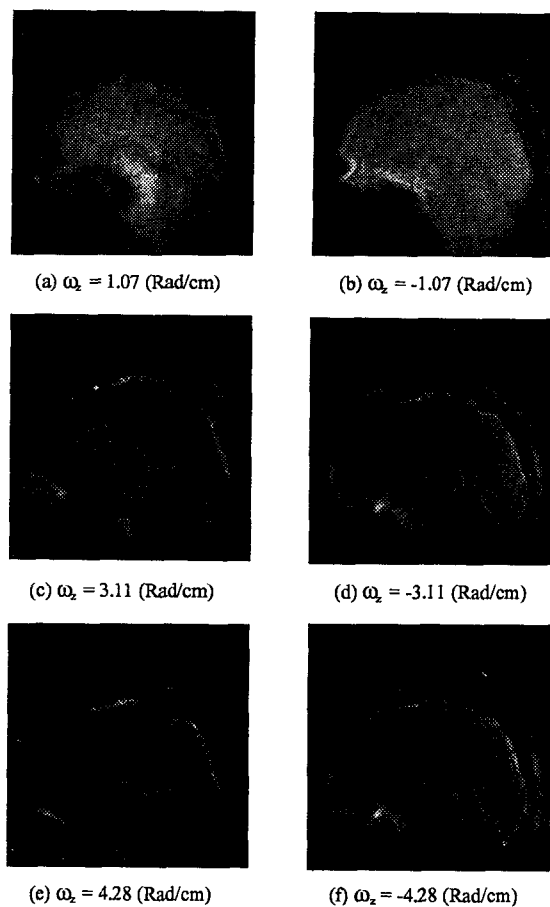(e) $\omega_z = 4.28$ (Rad/cm)

(f) $\omega_z = -4.28$ (Rad/cm)

Fig.6 Spectrally decomposed in-vivo human brain images. Each spectrally decomposed image,therefore,represents a susceptibility image of different susceptibility gradient strength. Note that the images at low spectral components such as $\omega_z = \pm 1.07$ (radian/cm) show the normal brain tissues while images at high spectral components such as $\omega_z = \pm 4.28$ (radian/cm) show the veins and tissue-vein interfaces where field gradients are strongest.